Electronic Supporting Information

1 MATERIALS AND METHODS

1.1 Endpoint staining

Devices were fixed by flowing 4% paraformaldehyde into the channels and leaving it for 10-15mins. When immunofluorescent staining for MT1-MMP was used, the devices were blocked with goat serum (Sigma G9023) for 2hr and MT1-MMP primary antibody in chicken (Sigma Cat. No. GW21125) was applied at 1:100 dilution ratio overnight at 4°C. The following day, Alexa Flour 568 goat anti-chicken (Invitrogen Cat. No. A11041) was flowed into the channels at a dilution ratio of 1:200 and incubated at room temperature for 2hr. Nuclei and F-actin were stained with 1μM Hoeschest 33342 (Invitrogen Cat. No. H3570) and either Alexa 488 Phalloidin (Invitrogen Cat No. A12379) or Rhodamine Phalloidin (Invitrogen Cat. No. R415) for 30-60min.

1.2 Imaging

Fluorescent stains were imaged on either an Olympus FV1000 (Olympus America – Center Valley, PA) inverted confocal microscope (live cell and fixed images using Rhodamine Phalloidin), or an Olympus IX81 wide field fluorescent microscope (images using Anti-MT1-MMP and Alexa 488 Phalloidin). A 20X objective was used in both cases. Because the wide field images suffered from a lot of out of focus background light, a background subtraction was used in ImageJ (NIH, USA) using a rolling ball radius of 20μm. All fluorescent images were rendered in Imaris 7.1 (Bitplane, AG –Zurich, Switzerland). Phase contrast images were taken using either an Olympus IX81 or an Olympus CX31 using a 10X phase objective.

1.3 Measurement of nascent vessels

The diameter measurements reported in Fig. 1D were selectively measured from confocal images of nascent vessels with a geometry consisting of an approximately straight centerline, had diameters that had less than 20% variation along their lengths, and had less than 20% difference between the measurements of *xz*-diameter and *xy*-diameter (see Fig. S3). The reported diameter values are the means of the *xy*-diameter along the length of the centerline. Reported elongation speeds, were computed as

$$v = \frac{\text{measured length}}{\text{experiment duration}} \tag{S1}$$

Due to the large number of data needed to compute the statistical responses to multiple MMP inhibitors and limited confocal microscope availability, the data in Figs. 2,S1 were measured from 2D phase contrast images and taken as the mean value from intact vessels like those shown in Figs. S1A-S1D.

1.4 Computational modeling

The computational model was implemented in COMSOL Multiphysics 4.2 with the chemical reaction toolbox (COMSOL - Burlington, MA) and simulation analysis was conducted in MATLAB (MathWorks, Inc. - Natick, MA). Analysis of the steady state elongation behavior was conducted using 2D axisymmetric coordinates, infinite boundary conditions, and <3μm triangular mesh size. The PARDISO algorithm was used. Simulations conducted for comparison with endpoint data implemented the full 3D post geometry (Fig. S4A) with no flux boundary conditions, and <3μm triangular mesh size. The 3D simulations used the Biconjugate Gradient Stabilization Method.

1.5 Quantitative analysis

The experimental endpoint sprout volume was determined in Imaris 7.1. A surface was fit to the Phalloidin 3D image using a surface feature resolution of 8μm in Imaris. The endpoint vessel centerline was determined in MATLAB and combined with the vessel tip locations from the phase contrast time points to determine the tip cell spatiotemporal trajectory. The trajectory was imported into the COMSOL simulation as the model input, Eq. (3). The resultant endpoint vessel profile was exported from COMSOL and compared against the experimental observation (Fig. S4). Since the Imaris surface fit consistently overestimated the cross-sectional area, the experimental cross section was periodically manually measured along the vessel length, s, in ImageJ. The simulated vessel was taken as the region where $c\left(\mathbf{x},t_f\right)<0.15c_0$.

2 QUANTITATIVE EVALUATION

We quantitatively evaluated the percentage error between the total simulated vessel volume V_S and experimental volume V_E as

$$\varepsilon_V = \left| \frac{V_E - V_S}{V_E} \right| \times 100\% \tag{S2}$$

The previous metric does not capture the spatially distributed nature of the vessel geometry. Therefore, we also evaluated the percentage root mean square (RMS) error between the experimental and simulated cross sectional diameters, $D_E(s)$ and $D_S(s)$. Integrating along the trajectory, with coordinate s (Fig. S4), yields

$$\varepsilon_A = \left(\frac{1}{s_f - s_0} \int_{s_0}^{s_f} \left(\frac{D_S(s) - D_E(s)}{D_E(s)} \right)^2 ds \right)^{1/2} \times 100\% \tag{S3}$$

where s_0 and s_f are chosen to eliminate measurement ambiguity at the base and tip of the vessel. In case the cross-section of the sprout is not perfectly round (typically happens when a sprout is growing along a PDMS or glass surface), we take $D = \sqrt{4/\pi A}$. We typically choose s_0 and s_f such that we evaluate greater than 70% of the vessel along its length, and approximate Eq. (S3) by measuring the sprout cross sectional areas along the length of the sprout based on the 3D phalloidin images. We evaluated the error of Sprouts 1-3 in Figs 4-5, yielding Table S1.

FIGURES

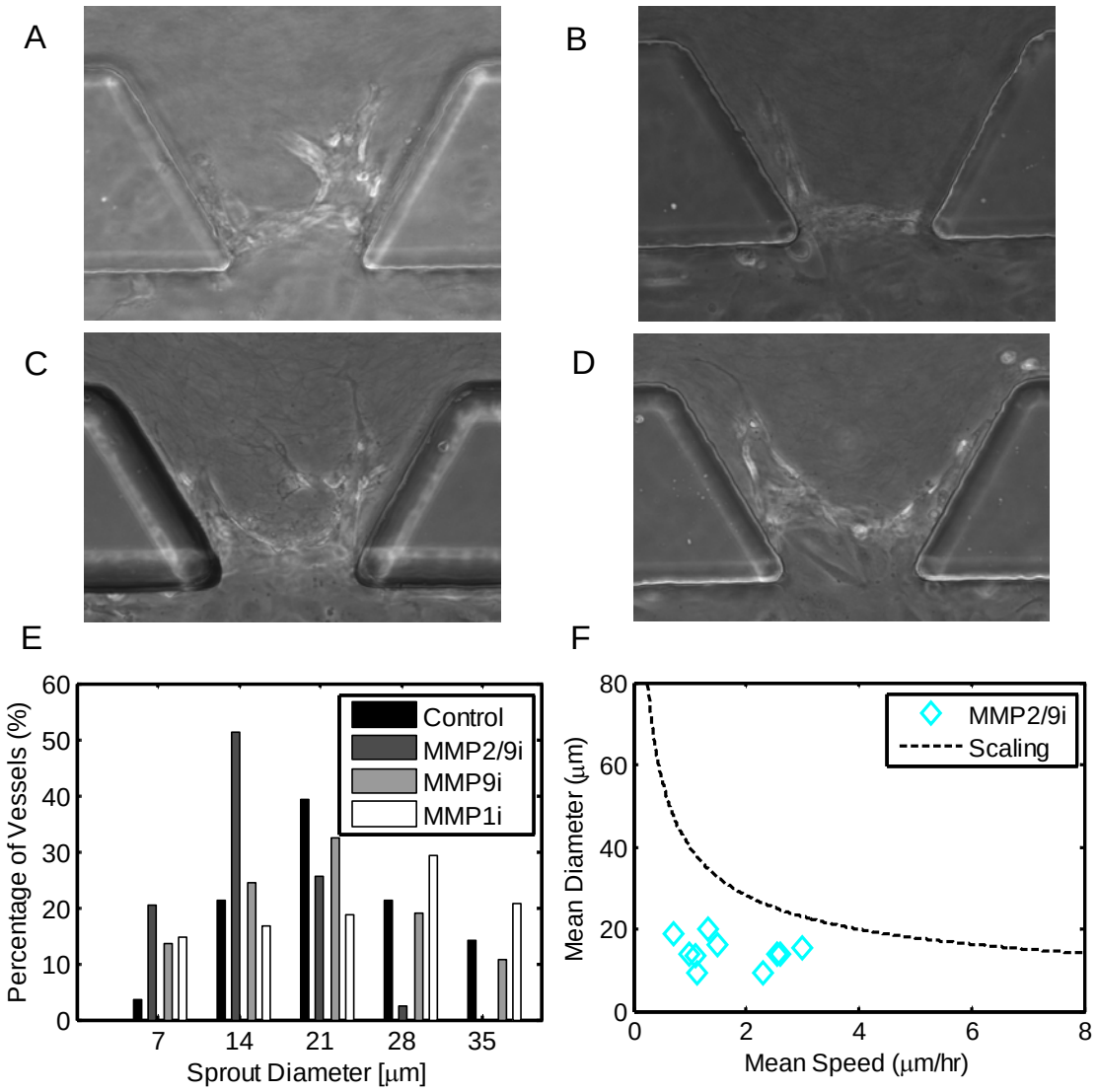

Fig. S 1: Influence of MMP inhibitors on sprout diameter with channel conditions [30ng/mL VEGF, 40ng/mL VEGF] over 72hr. (A) Phase contrast image of representative vessel from Control. (B) Representative vessel with 1μM MMP2/9i. (C) Representative vessel with 1μM MMP9i. (D) Representative vessel with 10μM MMP1i. (E) Histogram of all nascent vessel diameters measured after 72hr of growth for Control and each of the soluble MMP inhibitors. MMP2/9i shows a marked reduction in mean diameter and a reduction in variance of the distribution. (F) The MMP2/9i condition reduces vessel diameters without increasing elongation speed, meaning that observed growth (diamonds) do not hold to the $D_c \sim \sqrt{1/v}$ scaling relationship.

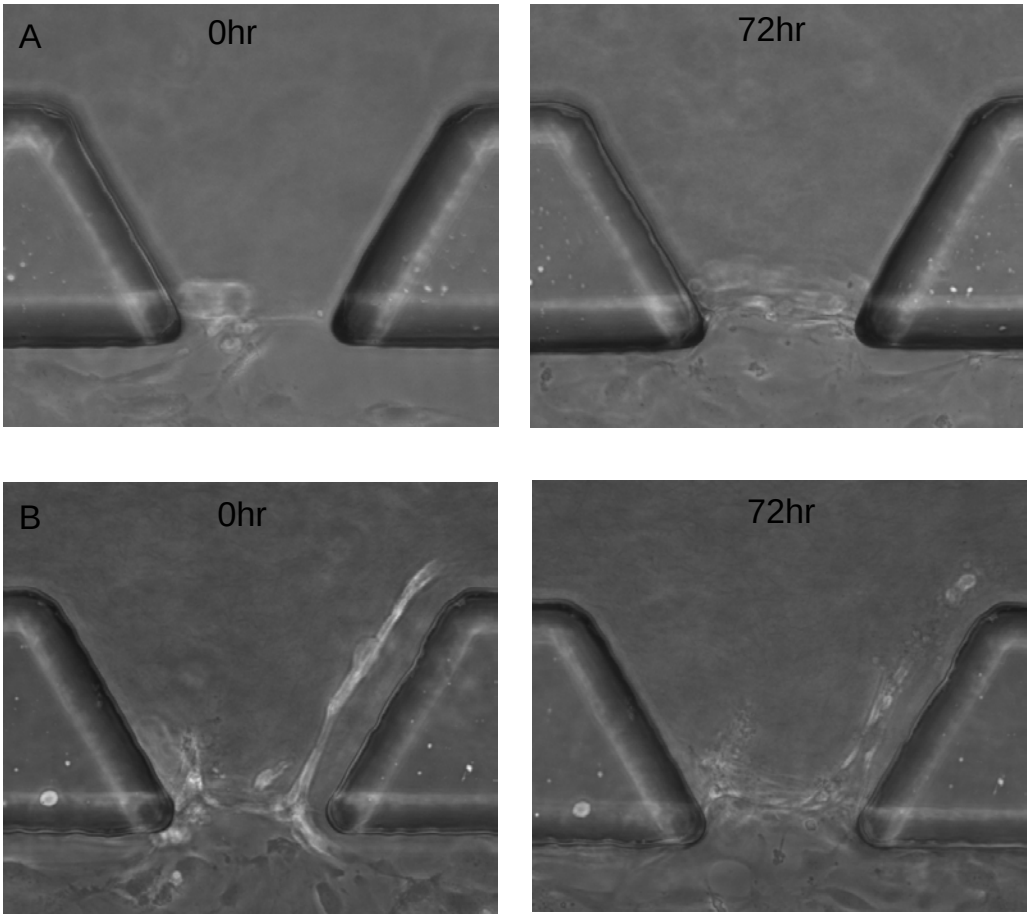

Fig. S 2: Nascent vessel response to 5μM pan-MMP inhibitor GM6001. (A) In stark contrast to inhibition of soluble species alone, pan-MMP inhibition lead to no vessel extension in any growth region that did not already have an existing tip cell. (B) Pan-MMP inhibition applied at 0hr in growth regions that had pre-existing nascent vessels halted vessel elongation.

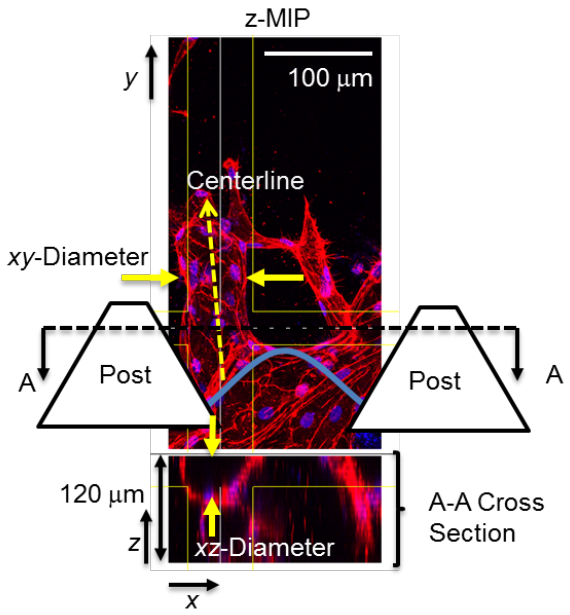

Fig. S 3 Illustration of diameter measurement procedure for data reported in Fig. 1D. The upper panel shows the *z*-direction maximum intensity projection (MIP) in the *xy*-plane while the lower panel shows the A-A cross section in the *xz*-plane. Measurements of mean diameter are taken from nascent vessels showing less than 20% variation in *xy*-diameter along their lengths and with less than 20% difference between the *xy* and *xz* diametric measurements. Red: Rhodamine Phalloidin. Blue: Hoechst 33342.

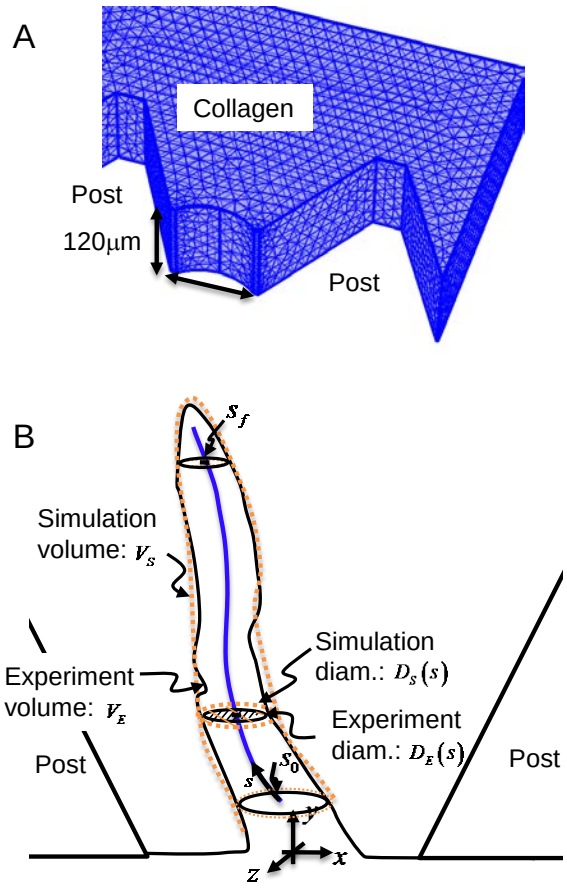

Fig. S 4: Computational modeling and data verification approach. (A) 3D mesh of computational model implemented in COMSOL. Model includes most geometry with no-flux boundary conditions on the top (PDMS surface of channel) and bottom (glass bottom of channel) and at the PDMS posts. (B) Illustration of comparison between simulation and experiment. The centerline of the final experimental volume is used as the simulated tip cell trajectory. The error between simulation and experiment was computed in terms of both total volume and root mean squared error in the cross sectional diameter. The cross was taken in the *xz*-plane. Volume and diameter were analyzed between the planes at s_0 and s_f to eliminate boundary errors due to unobserved MMP production as the tip cell is beginning to invade the gel and unrealized proteolysis at the tip due to endpoint fixation.

TABLES

TABLE S1: Simulation vs. experiment error metrics for Sprouts 1-3.

Metric	Sprout 1	Sprout 2	Sprout 3
Volume error, $\mathcal{E}_V$	1%	8%	3%
RMS diametric error, $\mathcal{E}_D$	14%	13%	7%